J|A|C|S COMMUNICATIONS

Published on Web 09/17/2010

Shape-Controlled Synthesis of Single-Crystalline Nanopillar Arrays by Template-Assisted Vapor−Liquid−Solid Process

Onur Ergen,[†,‡,§] Daniel J. Ruebusch,[†,‡,§] Hui Fang,[†,‡,§] Asghar A. Rathore,[†,‡,§] Rehan Kapadia,[†,‡,§] Zhiyong Fan,[†,‡,§] Kuniharu Takei,[†,‡,§] Arash Jamshidi,[†,‡] Ming Wu,[†,‡] and Ali Javey*[,†,‡,§]

Department of Electrical Engineering and Computer Sciences, University of California, Berkeley, California 94720, Berkeley Sensor and Actuator Center, University of California, Berkeley, California 94720, and Materials Sciences Division, Lawrence Berkeley National Laboratory, Berkeley, California 94720

Received June 15, 2010; E-mail: ajavey@eecs.berkeley.edu

Abstract: Highly regular, single-crystalline nanopillar arrays with tunable shapes and geometry are synthesized by the template-assisted vapor−liquid−solid growth mechanism. In this approach, the grown nanopillars faithfully reproduce the shape of the pores because during the growth the liquid catalyst seeds fill the space available, thereby conforming to the pore geometry. The process is highly generic for various material systems, and as an example, CdS and Ge nanopillar arrays with square, rectangular, and circular cross sections are demonstrated. In the future, this technique can be used to engineer the intrinsic properties of NPLs as a function of three independently controlled dimensional parameters - length, width and height.

In recent years, semiconductor nanowires (NWs) and nanopillars (NPLs) have been extensively explored for electronics, sensing, and energy applications.[1] Uniquely, their chemical and physical properties have been shown to exhibit a strong dependence on their dimensions, specifically the diameter and length, arising from various nanoscale phenomena.[2] Similarly, the cross-sectional shape and geometry of these nanostructures are expected to have an important effect on their properties. Yet, the controlled synthesis of single-crystalline NWs/NPLs with tunable shapes has not been well studied in part because the vapor−liquid−solid (VLS) growth mechanism often results in cylindrical structures as defined by the spherical shape of the catalytic seeds during the growth process.[3] In some instances noncylindrical nanowires have been observed; however these structures are highly material and process dependent and, therefore, do not offer the control necessary to engineer nanowire shape for an arbitrary material system.[4] Here, we utilize a template-assisted, VLS growth process[5] for the fabrication of highly regular and single-crystalline NPL arrays with tunable shapes, such as square, rectangular, or circular cross sections, as defined by the shape and geometry of the templates. The process is applied for the synthesis of CdS and Ge NPLs, presenting a generic platform toward the controlled synthesis of nanostructures with tunable shape and geometry.

Porous anodized alumina membranes (AAMs)[6,7] were used as the VLS templates (Figure 1), although the process scheme is generic for top-down fabricated templates as well. Briefly, the process scheme begins with the pretexturing of an electrochemically polished 0.25 mm thick aluminum substrate (99.99% Alfa Aesar) using a straight-line silicon diffraction grating as the mold. A two-step imprinting process was utilized to define the Al surface morphology, followed by an anodization step (Figures S1−S2). By varying the angle between the two imprint orientations and the pitch of the gratings, different indentation shapes can be formed on the aluminum surface, resulting in pores with different cross-sectional shapes following the subsequent anodization step. This control is enabled since the indentation regions formed by the overlap of the two imprinting steps act as nucleation sites for the pore development due to a local increase in the rate of field-enhanced dissolution of the oxide.[7] Figure 2 shows representative scanning electron microscope (SEM) images of the fabricated AAMs with square, rectangular, and circular pores with a pore depth of ∼1.6 μm. The figure demonstrates that the pore shape is accurately controlled over large areas. The pore depth is also well manipulated by the anodization time. A current ramping technique was then used to thin the alumina barrier at the bottom of the pores (Figure S3c) in preparation for a subsequent Au electrodeposition step (Figure S3d). The detailed process procedures can be found in the Supporting Information.

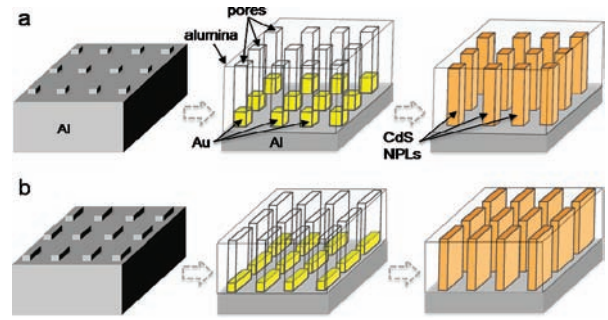

Figure 1. Process schematic for the template-assisted VLS synthesis of (a) square and (b) rectangular NPL arrays.

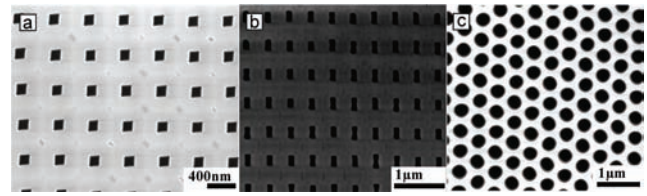

Figure 2. Top-view SEM images of the fabricated AAMs with (a) square, (b) rectangular, and (d) circular pores.

The electrodeposited Au is then used as catalytic seeds for template-assisted VLS growth of NPLs (see Supporting Information).[5] The process is generic for various NPL materials, and as an example, we demonstrate the shape-controlled synthesis of

[†] Department of Electrical Engineering and Computer Sciences, University of California.
[‡] Berkeley Sensor and Actuator Center, University of California.
[§] Lawrence Berkeley National Laboratory.

 10.1021/ja1052413

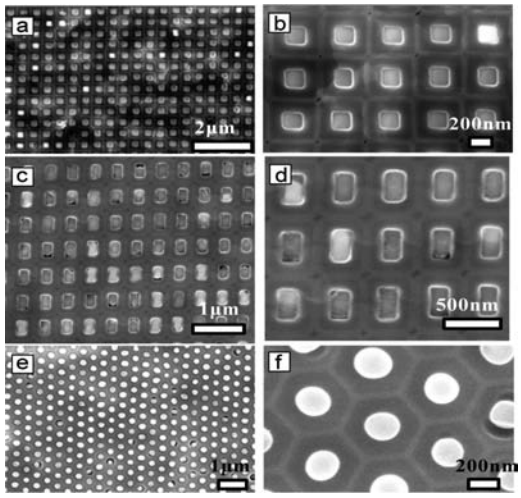

Figure 3. Top-view SEM images of highly ordered CdS NPLs with (a−b) square, (c−d) rectangular, and (e−f) circular cross sections, grown in AAM templates.

CdS (Figure 3) and Ge (Figure S4) NPLs. Figure 3 shows top-view SEM images of self-ordered pore arrays filled by indium-doped CdS NPLs with square (∼165 nm ×165 nm) (Figure 3a), rectangular (∼150 nm ×320 nm) (Figure 3b), and circular (∼250 nm diameter) (Figure 3c) cross-sectional shapes. The NPLs faithfully reproduce the shape of the pores because during the growth the liquid catalyst seeds fill the space available, thereby conforming to the pore geometry. To achieve this, sufficient gold must be deposited into the pores to ensure a complete filling of the cross-sectional pore area. If there is insufficient Au in the pores, spherical Au particles are formed during the growth, thereby resulting in the growth of cylindrical NPLs with diameters smaller than the width of the pores. Here, we have developed a simple geometrical argument to conservatively estimate the minimum thickness of Au necessary to achieve shaped controlled synthesis. A detailed discussion of this model can be found in the Supporting Information. The resulting relationships are

$$T_{Au} = ({}^{4}/_{3})R;\ T_{Au} = \frac{(x\pi\sqrt{2})}{3};\ T_{Au} = \left(\frac{\pi}{6xy}\right)(y^2 + z^2)^{3/2}$$

for the circular, square, and rectangular pores respectively, where T_{Au} is the Au thickness at the bottom of the pores, R is the radius of the circular pores, x is the width of the square pores, and y and z are the cross-sectional width and length of the rectangular pore. From our pore dimensions, we obtain a minimum Au thickness of ∼167, 222, and 480 nm for circular, square, and rectangular pores respectively. We note that in the template-assisted VLS mechanism, successful growth can be achieved as long as the gold thickness is more than the minimum values explained above (Figure S6), beyond which it has minimal effect on the growth.

The shape controlled synthesis process described here is also compatible with top-down fabricated templates. In this regard, we have fabricated fin-like Ge single-crystals (length ∼1.5 μm, width ∼380 nm, height ∼2 μm) on Si/SiO_2 substrates (Figure S5), demonstrating the potential utility of the scheme for heterogeneous and/or three-dimensional electronics on Si substrates. The rectangular nanopores used as templates were fabricated by electron beam lithography and dry etching of a ∼2 μm thick SiO_2 layer (Figure S5). Notably, a result of the growth process is that the NPL surfaces incorporate any roughness present on the pore sidewalls. The reliable production of extremely smooth pore sidewalls is needed, which is an inherent advantage of the AAM templates as compared to nanopores fabricated using top-down etching methods.

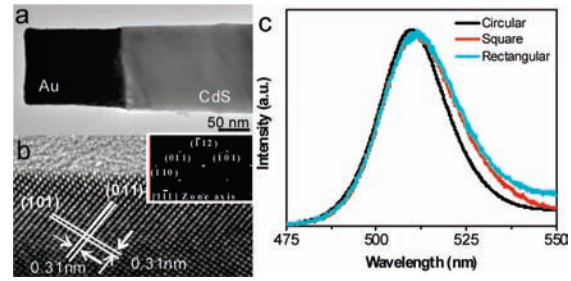

Figure 4. (a−b) TEM images of square-shaped CdS NPL, depicting its single crystalline structure. (c) PL spectra of square, rectangular, and circular CdS NPLs.

The crystal structure and materials quality of the shape-controlled CdS NPLs were characterized by transmission electron microscopy (TEM) and photoluminescence (PL) spectroscopy. The low magnification TEM image of a square-shaped CdS NPL with the corresponding electron diffraction pattern shows the single crystalline nature of the as-grown structures (Figure 4a). The Au catalytic seed is clearly depicted in the TEM image, which is a signature of the VLS growth. The high-resolution TEM image depicts the lattice fringes and preferred [110] growth direction (Figure 4a). The observed lattice spacing is the same as that for circular CdS NPLs.[5a] The PL spectra of the CdS NPLs (Figure 4b) illustrate band emission at ∼512 nm for different shape NPLs. There is no peak shift as compared to the previously reported bulk CdS value,[8] which is expected since the scale of the explored NPLs is still beyond the Bohr radius of bulk CdS (∼5 nm). In the future, NPLs with dimensions on the order of the Bohr radius can be synthesized and characterized to observe quantization effects and the corresponding divergence in the properties of NPLs of differing shapes. Successful scaling of this templated growth process presents significant challenges, including the formation of ∼5 nm pores with sharp corners and good wetting properties.

In summary, a versatile route toward the controlled synthesis of single crystalline NPL arrays with tunable shapes is demonstrated by a template-assisted VLS growth mechanism. The ability to control the cross-sectional geometry of NWs in addition to their dimensions provides yet another degree of control in exploring novel phenomena at the nanoscale and designing materials with the desired properties and functionalities.

Acknowledgment. This work was funded by BSAC and MDV. The synthesis part was supported by an LDRD from LBL. A.J. acknowledges support from World Class University program.

Supporting Information Available: Detailed information about AAM fabrication, alumina barrier thinning, NPL growth, and the minimal Au thickness required for a successful growth. SEM images after various process steps and for Ge NPL growth are also shown. This material is available free of charge via the Internet at http://pubs.acs.org.

References

(1) (a) Lieber, C. M.; Wang, Z. L. *MRS Bull.* **2007**, *32*, 99–104. (b) Javey, A. *ACS Nano* **2008**, *2*, 1329–1335. (c) Yang, P.; Fardy, M.; Yan, R. *Nano Lett.* **2010**, *10*, 1529.

(2) (a) Ford, A. C.; Ho, J. C.; Chueh, Y.-L.; Tseng, Y.-C.; Fan, Z.; Guo, J.; Bokor, J.; Javey, A. *Nano Lett.* **2009**, *9*, 360. (b) Ma, D. D. D.; Lee, C. S.; Au, F. C. K.; Tong, S. Y.; Lee, S. T. *Science* **2003**, *299*, 1874. (c) Tian, B.; Xie, P.; Kempa, T. J.; Bell, D. C.; Lieber, C. M. *Nat. Nanotechnol.* **2009**, *4*, 824.

(3) (a) Wagner, R. S.; Ellis, W. C. *Appl. Phys. Lett.* **1964**, *4*, 89. (b) Kodambaka, S.; Tersoff, J.; Reuter, M. C.; Ross, F. M. *Science* **2007**, *316*, 729.
(4) (a) Kuykendall, T.; Pauzauskie, P.; Lee, S.; Zhang, Y.; Goldberger, J.; Yang, P. *Nano Lett.* **2003**, *8*, 1063. (b) Wagner, V.; Parillaud, O.; Buhlmann, J.; llegems, M. *J. Appl. Phys.* **2002**, *92*, 1307.
(5) (a) Fan, Z.; Razavi, H.; Do, J.; Moriwaki, A.; Ergen, O.; Chueh, Y.-L.; Leu, P. W.; Ho, J. C.; Takahashi, T.; Reichertz, L. A.; Neale, S.; Yu, K.; Wu, M.; Ager, J. W.; Javey, A. *Nat. Mater.* **2009**, *8*, 648. (b) Fan, Z.; Kapadia, R.; Leu, P.; Zhang, X.; Chueh, Y.-L.; Takei, K.; Yu, K.; Jamshidi, A.; Rathore, A.; Ruebusch, D.; Wu, M.; Javey, A. *Nano Lett.* **2010**, ASAP (DOI: 10.1021/nl1010788). (c) Lew, K. K.; Reuther, C.; Carim, A. H.; Redwing, J. M.; Martin, B. R. *J. Vac. Sci. Technol. B* **2002**, *20*, 389.
(6) (a) Masuda, H.; Fukuda, K. *Science* **1995**, *268*, 1466. (b) Masuda, H.; Asoh, H.; Watanabe, M.; Nishio, K.; Nakao, M.; Tamamura, T. *Adv. Mater.* **2001**, *13*, 189.
(7) (a) Parkhutik, V. P.; Shershulsky, V. I. *J. Phys. D: Appl. Phys.* **1992**, *25*, 1258. (b) Lee, W.; Ji, R.; Ross, C. A.; Goselle, U.; Nielsch, K. *Small* **2006**, *2*, 978.
(8) Perna, G.; Capozzi, V.; Ambrico, M.; Augelli, V.; Ligonzo, T.; Minafra, A.; Schiavulli, L.; Pallara, M. *Thin Solid Films* **2004**, *453*, 187.

JA1052413